Static laser weeding system based on improved YOLOv8 and image fusion

Xiwang Du, Xia Li, Fangtao Duan, Jiawei Hua, Mengchao Hu

School of Mechanical Engineering, Tianjin University of Technology, Tianjin, China

Abstract

Laser weeding is one of the promising weed control methods for weed management in organic agriculture. However, the complex field environments lead to low weed detection accuracy, which makes it difficult to meet the requirements of high-precision laser weed control. To overcome this challenge and facilitate precise weeding by laser weeding robots in complex fields, this study suggests the use of a dual-mode image fusion algorithm of visible light and infrared light based on machine vision. This innovative technology, introducing infrared information based on visible light images, enhances weed detection accuracy and resilience to environmental factors. The introduction of the Swin-transformer module and Slim-neck module enables the creation of a brand new weed detection model allied with the YOLOv8 model, applicable for weed meristem detection. According to the experimental results, for fusion images with a resolution of 640*640, the dual-scale fusion of RGB and NIR images on the improved network has an average accuracy (mAP) of 96.0% and a detection accuracy of 94.0%, respectively. This study builds a laser weeding robot with a mobile platform, a weed recognition module and a laser polarization transmitter module. The ROS system is utilized to effectively detect weeds and determine their geometric center position after the weed detection model is successfully installed on the robot platform. The laser vibrator demonstrates accurate deflection to the weed growth position during the weed detection and laser illumination experiment. The results show that the accuracy of weed detection has reached 82.1%, and the efficiency of laser weeding has reached 72.3%. These results prove the feasibility of the laser weeding method proposed in this study. However, the fusion strategy of these two kinds of images still has great room for improvement in terms of detection accuracy and efficiency. In the future, multiple modal information can be used to improve the identification efficiency of weeds in the field.

Correspondence: Xia Li, School of Mechanical Engineering, Tianjin University of Technology, Tianjin, 300384, China.
E-mail: lixia0415@email.tjut.edu.cn

Key words: Image fusion, deep learning, weed detection, laser weeding.

Conflict of interest: the author declares that there are no known competitive economic interests or personal relationships that affect the work reported in this article.

Availability of data and materials: the data that support the findings of this study are available from the corresponding author upon reasonable request.

Acknowledgements: we appreciate the weed dataset provided by the Bonn Institute. This work has received partial funding from the National Natural Science Foundation of China (NSFC) 32171902 and 32060417. Received funding from the School of Mechanical Engineering at Tianjin University of Technology project (YJ2306).

Received: 31 January 2024.
Accepted: 22 August 2024.

Journal of Agricultural Engineering 2024; LV:1598
doi:10.4081/jae.2024.1598

Introduction

Many countries' economic development is largely dependent on their agricultural advancement (Bwambale *et al*., 2022) and the primary cause of resource loss and decreased crop output is the presence of weeds (Fahad *et al*., 2015; Jiang *et al*., 2023). Therefore, one of the longest-standing issues in agricultural science has been how to successfully limit weed development (Wu *et al*., 2020; Raja *et al*., 2020). Herbicides have been used extensively since their invention and are currently the most common and effective means of controlling weeds (Wang *et al*., 2023; Westwood *et al*., 2018), but their pollution to the ecological environment cannot be ignored (Sujaritha *et al*., 2017), and when used repeatedly, they not only make weeds more resistant to control (Zhu *et al*., 2020; Machleb *et al*., 2020), but also present a risk to human health (Rani *et al*., 2021). Furthermore, there is little financial gain from the time-consuming and labor-intensive traditional manual weeding method. The automation of farmland weeding is the key step to solving the problem of farming drug damage, increasing weeding efficiency, and boosting the financial gain from agriculture. Despite the fact that automated weeding techniques, such as automated targeted sprayers, can minimize the application of herbicides, the weeding outcome is subpar due to fog drift and poor adhesion caused by weather factors in targeted spray weeding methods (Ahmad *et al*., 2018; Zou *et al*., 2023). The herbicide dosage is reduced but the weeding effect is poor. In addition, non-chemical automatic weeding methods such as mechanical weeding and flame weeding are also employed in a certain range. While mechanical weeding is very effective and low-impact on the environment, in-line weeding can harm crops and eradicate weeds that are too close to them. Weeding at the small and vulnerable stage will cause irreversible damage to

seedlings (Perez-Ruiz *et al*., 2014; Quan *et al*., 2022). The flame weeding method (Martelloni *et al*., 2020) mostly relies on heavy machinery, resulting in certain soil compaction and making accurate weeding impossible. Therefore, exploring efficient and eco-friendly automated weeding technology in farmland is becoming the main focus of achieving harmless weeding.

In recent years, laser technology has been widely studied as a more advanced and eco-friendly weeding technique. With its high efficiency, low damage rate, low pollution, and great adaptability, laser weeding is a precise non-contact weeding technology that can be used without touching the soil or crops. However, it does require a robotic system that can autonomously detect and remove weeds. The automation of farm operations will promote agricultural intelligence, boost production efficiency and increase economic benefits. Xiong *et al*. (2017) built a laser weeding robot to plan the laser weeding path in a region for static weeding. Zhu *et al*. (2022) developed a blue laser weeding robot based on YOLOX to identify and target weeds, employ blue lasers with increased laser energy, and study the lethal laser energy of various weeds. Wang *et al*. (2022) designed a two-degree-of-freedom head to meet the requirements of laser weed removal with high precision and dynamic performance. At 0.1/s speed, the weed removal efficiency was 0.72 s/ plant and the dwell duration was 0.64s. Arsa *et al*. (2023) proposed a convolutional neural network based on encoder-decoder to train the labeled weed centroid, forecast the location of weed meristem directly, and achieve the precise strike of laser weeding by using laser irradiation.

In addition, weed detection in the field is a difficult undertaking. The complicated and variable illumination conditions in the outdoors cause weed identification accuracy to be lower than in an indoor setting (Wang *et al*., 2019). A complex field environment makes it difficult to rapidly and effectively detect weeds because of the strong light irradiation, uneven light, and shadow that can cause significant reflection on the overall or local surface. Furthermore, early weed detection is essential to minimizing the usage of herbicides and averting large losses of agricultural resources (Espejo-Garcia *et al*., 2023). Thus, the key to enhancing early weed detection effectiveness in complicated field environments is to explore ways to reduce the influence of environmental factors and enhance algorithmic detection performance in the field weeding process. Increasing the effectiveness of weed detection is a crucial step toward increasing production efficiency and financial gains as well as supporting the intelligent and mechanized agricultural production.

At present, field weed detection mainly relies on single-mode images obtained by a single sensor, which has limited information and poor adaptability (Li *et al*., 2021). When detecting small-size weeds or weeds with low contrast, single-mode images are often difficult to achieve effective detection. Moreover, the anti-interference strength and accuracy cannot meet the high standards of precision agriculture (Cisternas *et al*., 2020). The detection performance of single-mode systems, especially visible light images, is easily affected by changes in lighting conditions. In addition, single-mode infrared images or other images with similar modes may lead to incomplete image information in cloudy, rainy or foggy days, thus reducing detection efficiency. The advantage of image fusion creates a new path for the development of target detection and has been extensively researched and applied. Li and Wu (2019) proposed a deep learning model based on CNN and dense blocks to solve the fusion problem of infrared and visible images, which had advanced fusion performance. Tu *et al*. (2020) proposed a multi-scale fast regional convolutional neural network to fuse color images and depth images in order to detect fruits under variable illumination, severe occlusion and low resolution. Gan *et al*. (2018) used a thermal camera and a color camera to establish a multimodal system to detect immature green citrus fruits. Compared with color images alone, the image fusion of the two cameras improved the fruit detection ability. Xu *et al*. (2021) fused visible light and depth images, taking into account mutual independence and complementarity, and realized the fusion of multi-mode information at the decision-making level, thus enhancing the performance of weed detection despite the restricted information of single-mode images. Li *et al*. (2023) built an interactive attention module and extracted association information and the boundary line of farmland headlands using the time series information processing module by complementing the features of RGB images and depth images. Gai *et al*. (2020) proposed an image processing pipeline that fused color and depth images to detect and locate broccoli and lettuce plants. Therefore, the application of image fusion technology to the agricultural field can increase the accuracy of target recognition and improve the efficiency of agricultural automatic production. However, research on fusion methods for picture fusion technology is still in its infancy, making its application in agriculture difficult.

The key to improving target detection precision is to adopt an effective feature image fusion technique. Therefore, in order to address the issue of low recognition efficiency and accuracy in field weed detection due to environmental factors, this study adopts a pixel-level image fusion technique based on dual-scale image fusion to fuse visible light (RGB) and infrared light (NIR) images captured by laser weeding robots. Weather and variations in light have little effect on NIR images (Xue *et al*., 2021). RGB images are rich in color and contain abundant weed edge and detail information, which are complementary to NIR images and almost perfectly capture the natural characteristics of weeds (Ma *et al*., 2019), thus improving the reliability and accuracy of weed detection (Zhang *et al*., 2020). The use of image fusion to fuse visible and infrared images is an effective strategy to improve the performance of field weed detection systems, especially in the face of different weather and light conditions. This fusion technique significantly enhances the robustness and accuracy of the system by combining the advantages of both image modes. Specifically, visible light images provide rich color and texture information to help identify plants and weeds in good lighting conditions; The infrared image captures the temperature difference between the plant and the background, and is less affected by environmental factors such as rain and fog, which can provide clear images under these conditions and maintain detection performance. In addition, the Swin-transformer model is utilized to better understand the context between the RGB and NIR fused images, and to extract the local and global features in the images more efficiently, so as to improve the accuracy of weed detection in the field environment. On this basis, a mobile platform for automatic end-laser polarization weeding is developed to accurately pinpoint the weed's meristem (Mathiassen *et al*., 2006) and trigger laser irradiation, which is of great significance for enhancing the efficiency of weeding and minimizing resource waste. Concurrently, the effectiveness of the multi-mode fusion laser weeding approach is assessed in the field environment, and its potential use in agricultural production is explored.

This paper's remaining content is as follows: the second section overviews the process of creating a dataset and bimodal image fusion, and enhances and optimizes the YOLOv8 network architecture, particularly in terms of improving the capability to detect small target weeds and locating their meristem. The weeding robot's control system, comprising the flow design of the control

system and the introduction of the laser galvanometer system, is designed in the third section. The fourth section carries out the field experiment and analyzes the comprehensive experiment results. The fifth and final section provides a summary of the study's primary findings as well as recommendations for future research directions.

Materials and Methods

In order to realize the systematic implementation of precise weeding by combining deep learning object detection model with laser weeding technique, this study will tackle aspects such as image data set creation, dual-mode image fusion, target detection model construction and improvement to improve field weed detection performance. After that, field tests of laser weeding will be conducted to confirm the viability of weed detection by laser weeding method and dual-mode image fusion, as well as hardware construction and model deployment of the laser weeding robot. The overall process of this study is shown in Figure 1.

Crop and weed detection based on YOLOv8

Data acquisition and dataset creation

Two weed image datasets are employed in this study. The first one is the German Bonn Beet dataset, a dataset of beet images that is publicly available (http://www.ipb.uni-bonn.de/data/sugarbeet-s2016/) and takes the data set as the pre-training of the image. The second type of data set is the data set taken by the research group in the corn field of Kexin Agricultural Base, Xiqing District, Tianjin on July 10, 2023, using Intel realsense camera D435i (Intel, USA) at a fixed height. The dataset has fewer images and more unstructured factors in the complex field environment. In addition, the light intensity is strong and there is a large interference during shooting. The research carried out shading processing on the image shooting device, and used 8 fill lights to manually fill the light to ensure the shooting quality of the data set. In order to obtain a large amount of detection data of laser weeding robot in the field, image acquisition was conducted from the human perspective and the height consistent with the visual detection system of laser weeding robot. The depth camera was used to shoot vertically down 90°, which is the normal configuration of field weeding. At the same time, the video stream information of weeds and plants is collected, and images can be extracted to enrich the data set. Due to the limited amount of data in the second dataset images, the Beet dataset from Bonn, Germany is intended to be used for training the research network, and the transfer training strategy is adopted for the self-shot dataset to enhance the model accuracy. The dataset includes images of beet taken over three months at various growth stages, times, and light intensities, and the shooting angle is fixed. However, due to the poor quality of some images, 809 images are selected from the 2,000 images as the dataset for this study, resulting in 809 RGB images (1296*966) and 809 corresponding infrared images (1296*966).

In this study, LabelImg software is used to manually label image frames and labels for crops and weeds in the images. yolo format is used as output, COCO format is adopted, and the images are divided into two folders: Images and Labels, with Images storing the images and Labels storing the txt format files of the corresponding images. Because the infrared image coincides perfectly with the visible image, labeling is valid for both types of images.

Dual-scale image fusion

Conventional machine vision techniques mostly rely on a single sensor to gather data; however, they are unable to meet precision agriculture's demands for accuracy in real time. In contrast, multi-modal image fusion technology can greatly enhance detection performance by fully utilizing complementary information from various data sources. According to the different processing levels, image fusion technology can be divided into three kinds: pixel-level fusion, feature-level fusion and decision-level fusion. Pixel-level fusion is based on strict image registration, which directly synthesizes each sensor's output data to create a fusion image with additional information. Compared with feature-level fusion and decision-level fusion, pixel-level image fusion has advantages in detail information richness, generalization capability, data stability and flexibility of image fusion strategy (Li *et al*., 2021). Studies have shown that the early stage of image fusion is particularly effective for small target detection (Cheng *et al*., 2023). Therefore, in order to enhance the information in the images, this study applies the pixel-level dual-scale image fusion approach (Bavirisetti and Dhuli, 2016) and fuses the 809 visible and 809 infrared images acquired in accordance with the complexity of the field environment and the volume of information, resulting in 809 images with two different types of data. The visible light and infrared light are fused by the following steps: The pixel-level fusion method may introduce redundant information and noise during image fusion. First, the input visible light image and infrared image are filtered by means of average filtering, and the average filtering coefficient is 35, so as to remove random noise in the image, retain the main structure and color information, and obtain the base layer image. Then, by subtracting the filtered image from the original image, the detail layer image containing high-frequency information is obtained, and the difference between the two represents the detail information contained in the image. Then, the original image is processed by median filtering, and the median filtering coefficient is 3. Then the error calculation is carried out to calculate the difference between the median filtered image and the mean filtered image, and a small constant of 0.01 is added to avoid the division by zero error. The weight of each pixel is calculated based on the error, thereby merging the layers of detail. After the above steps are completed, the image fusion operation is carried out. First, the average value of the two base layers is fused, which is used as the fused base layer. According to the weight information calculated by the above steps, the detail layer is merged. The fused image is shown in step 1 of Figure 1.

Data augmentation and partitioning

Data augmentation is a key technique in the field of computer vision, which aims to enrich the training set by increasing the diversity and quantity of data, thereby improving the robustness and generalization capability of the model. In this study, we used Python for data augmentation, including improving image brightness, adding noise, etc., to further enrich the training set of weeds and crops. After data augmentation, a total of 2427 images are obtained. In order to evaluate the performance of the model, the enhanced dataset is randomly divided into a training set, a validation set and a test set at a ratio of 8:1:1. Specifically, 1,941 images are used for training, 242 images for validation, and 244 images for testing.

Improved weed detection model based on YOLOv8

This study constructs a deep learning network to precisely identify weeds in the field, utilizing the advantages of pixel-level

image fusion to manage the complexity and vast amount of information in the field environment for accurate weed identification. In order to more efficiently extract weed data from the fused images, this study employs the YOLOv8 network to fulfill the training and detection tasks following the image fusion, in line with field real-time prerequisites. The YOLO series is widely used and has demonstrated remarkable performance in routine target detection tasks, especially its speed, ease of deployment, and high-precision features make it a popular choice in the agricultural sector. However, the performance can be limited when faced with challenges such as small target features, low-resolution images, blurred target details, and complex scenes after dual-modal image fusion. Due to the tiny size, similar color and characteristics of weeds and crops, and the influence of light and shadow, the YOLOv8 network's weed detection performance in field environments needs to be further enhanced, particularly for weed detection and localization in the maize seedling stage. To solve the above problems, we choose the YOLOv8 network as the foundational network framework, improve the YOLOv8 network by incorporating the Swin-transformer module, and employ the Slim-neck module to boost the neural network's effectiveness and performance. The converged network structure, as shown in Step 2, is depicted in Figure 1. YOLOv8 is composed of the backbone network, neck network and detection head. The neck network and detection head forecast the boundary box and label of the object in the feature map, while the backbone network is in charge of extracting image features from the input image. In order to improve the efficiency of weed detection in the field, the minimum weight model of YOLOv8 is selected for pre-training.

Swin-transformer network

As shown in step 2 in Figure 1, in particular, we replace YOLOv8's original backbone with Swin-transformer's backbone. The introduction of the Swin-transformer module aims to improve the network's processing capability for small target features, low-resolution images, blurred target details and complex scenes after dual-mode image fusion, so as to improve the detection performance of weeds in the field. We will perform a comprehensive performance comparison of the improved network to verify its performance improvement. Swin Transformer, as a windowing multi-head self-attention module, has a similar image feature extraction capability as convolutional neural networks (CNNS). As a result, it can serve as the backbone network needed to successfully complete the target detection task. The input image is first divided into multiple small blocks by the PatchEmbed module, and these blocks are then embedded in the high-dimensional vector. SwinStage includes the Patch Merging module and multiple Swin Transformer Block modules, and calculates the self-attention of multiple small blocks by employing the hierarchical attention mechanism. MLP is then used to process the output and extract higher level features. The PatchMerging module creates a new vector by fusing the adjacent small blocks to form larger chunks. The input is effectively subsampled n times by the formula (H/n) x (W/n) x (2nC), where H, W, and C in step 2 of Figure 1 represent height, width, and channel depth, respectively.

Lastly, the SPPF module is used for feature processing, which can effectively extract multi-scale features of the image. Consequently, the addition of the Swin transformer module, which is effective at detecting small targets, is chosen to increase the precision and speed of weed detection.

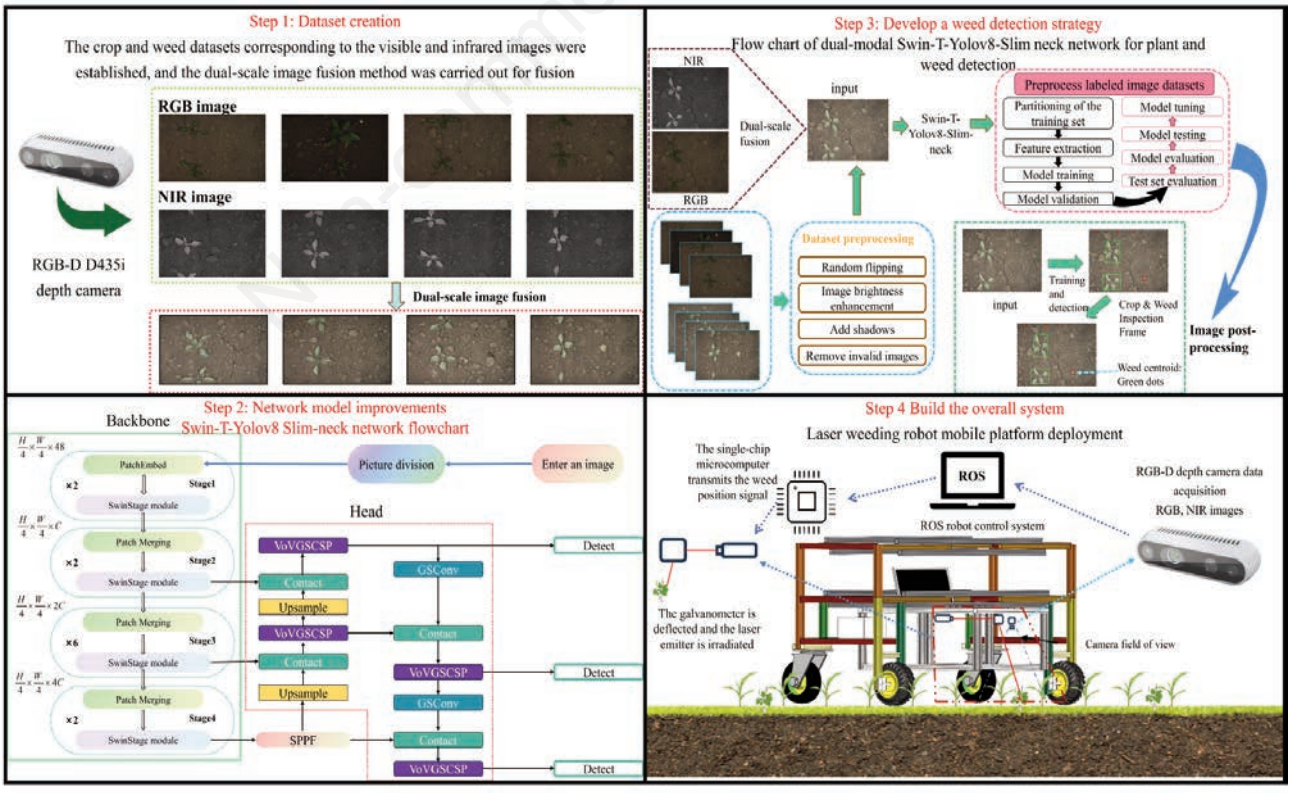

Figure 1. Overall flowchart of the study.

Slim-neck module

In this study, the backbone network of YOLOv8 is optimized to improve its target detection ability. Then, the Slim-neck module is introduced to lightweight the Head layer of YOLOv8. This mainly consists of GSconv, GS bottleneck and VoV-GSCSP modules, which are introduced to improve the ability of feature fusion and processing, so as to improve the detection accuracy of small target weeds. The introduction of the GSConv module is to solve the problem of predictive computing speed in the convolutional neural network and decrease temporal complexity, The model is shown in Figure 2. The GS bottleneck module is used to enhance nonlinear expression and information reuse. VoV-GSCSP module is a new lightweight model, which is a cross-level partial network built by one-time aggregation and consists of the widely used lightweight network structure VoV Net and CSP Net, The model is shown in Figure 3. By using the VoV-GSCSP module in place of the original residual structure C2f in the Head layer, the network model's lightweight nature is achieved, and the computation cost is significantly decreased. At the same time, this improvement maintains the accuracy of the network model to a certain extent and fulfills the detection criteria. This structural improvement can achieve the lightweight of the model and guarantee the accuracy of the detection.

Model training environment and training methods

In order to achieve more accurate target detection, this research selects a deep learning framework based on PyTorch architecture for image processing and model training. The experimental environment is configured as follows: Python version 3.8, CUDA 11.7 is used for parallel computing, and cuDNN 11.0 is used as a GPU acceleration library. The experiment ran on a Windows 11 operating system with hardware configurations including an NVIDIA RTX3050 GPU (4GB) and an Intel (R) Core (TM) i5-12500 (2.7GHz) CPU. In the network training process, the number of training rounds is set to 200, the initial learning rate is set to 0.01, 16 sample graphs are randomly selected for each batch, the SGD dynamic gradient descent method is adopted, and the model momentum parameter is set to 0.937 (Table 1).

Furthermore, in order to accurately identify weeds in corn fields, this study employs a transfer learning technique to transfer the pre-trained model weights to actual field detection tasks. Due to the challenge of obtaining large amounts of annotated data in specific agricultural environments, transfer learning provides a solution that allows us to significantly minimize the amount of annotated data required by utilizing pre-trained models on huge datasets. In addition, as the model has already acquired many useful features on the source task, transfer learning can also help shorten training time and improve model performance when the target task has a small amount of data. The pre-training of the model on the source task allows it to acquire more broadly applicable features that can improve its performance on the target task.

Evaluation indicators

In order to comprehensively evaluate the performance of our proposed Swin-T-YOLOv8+Slim neck model in weed detection tasks, we use multiple evaluation indicators to verify its effectiveness. Firstly, we adopt average accuracy (map@0.5) as the main evaluation indicator. map@0.5 is an important evaluation metric for object detection algorithms, which measures the average accuracy of the model at a threshold of Intersection over Union (IoU) of 0.5. The mAP value is obtained by calculating the area under the Precision Recall curve, and the higher the mAP value, the better the detection performance of the model. Calculation of mAP requires Precision and Recall of model training samples, as shown in formula (1) and (2):

$$\text{Precision} = \frac{TP}{TP + FP} \quad (1)$$

$$R = \frac{TP}{TP + FN} \quad (2)$$

In the above formula, TP is true positives. If the prediction result is true (pair), the true value is positives (positive example) and the model considers them as positives (positive example). FP is a false positive example, the prediction result is false (wrong), the true value is negative (negative), the model considers it to be positives (positive), FN (false negative) indicates that the target has not been correctly detected.

By calculating the area below the accuracy-recall curve (P-R curve) formed by the ordinate Precision and the abscissa Recall, the average precision nAP of the target category can be obtained, as shown in formula (3) :

$$n_{AP} = \int_0^1 P_{\text{recision}}\, dR_{\text{ecall}} \quad (3)$$

mAP can be obtained by averaging the average accuracy of n categories, as shown in formula (4):

Table 1. Hyperparameter settings.

Hyperparameter settings	Value
Batch size	16
Epochs	200
Initial learning rate	0.001
Momentum	0.937

Table 2. Comparison of parameters between YOLOV8 and the improved Swin-T-YOLOv8+Slim neck under different modes.

Method	Type	Precision	Recall	mAP0.5	FPS
Swin-T YOLOv8+Slim-neck	RGB+NIR	0.940	0.920	0.960	120
Swin-T YOLOv8	RGB+NIR	0.936	0.915	0.955	115
YOLOv8	RGB+NIR	0.814	0.846	0.933	114
YOLOv8	RGB	0.802	0.883	0.893	112
YOLOv8	NIR	0.842	0.839	0.910	120

$$mAP = \frac{1}{n}\sum_{i=0}^{n} n_{AP_i} \quad (4)$$

Where: n is the total number of categories in the training sample dataset, and i is the current category number.

These indicators can provide us a basis for further model optimization by giving us a more thorough understanding of the model's performance in weed detection tasks.

Ablation experiment

In order to verify the efficacy of our dual-mode weed detection and the improved Swin-T-YOLOv8+Slim-neck model, we use this dataset to compare the results with those of the single-mode training. As shown in Table 2, we select a variety of parameters for comparison to fully evaluate the performance of the model. Specifically, we compare the YOLOv8 model with RGB and NIR images as inputs, the YOLOv8 model with RGB and NIR image fusion, and our proposed Swin-T YOLOv8 model. Through contrastive analysis, we verify the effectiveness of bimodal image fusion and the performance of the improved network model.

The experimental data are shown in Table 2. Three experiments were conducted for each model adopted in the table, and the result of one of the best results among the three experiments of each model was used as the representative parameter of this experiment. The results indicate that the improved Swin-t YOLOv8 mAP has a higher score (0.9553) than the four different types of the unimproved YOLOv8 network (dual-mode, RGB single-mode, and NIR single-mode) when compared to the original network. The dual-mode training results of the improved Swin-T-YOLOv8+Slim-neck module are improved by 0.5% compared with Swin-T-YOLOv8 network dual-mode accuracy, 2.7% compared with YOLOv8 network dual-mode accuracy, 6.7% compared with RGB single-mode accuracy, and 5% compared with NIR single-mode accuracy. Furthermore, in terms of detection accuracy index, the improved Swin-T-YOLOv8+Slim-neck dual-mode improves by 0.4% compared with Swin-T-YOLOv8 network dual-mode accuracy, 8.5% compared with RGB single-mode accuracy, and 10.4% NIR single-mode accuracy. In terms of Recall value, the parameter value of the improved Swin-T-YOLOv8+Slim-neck model also performs the best, reaching 92.0%. Compared with the Swin-T-YOLOv8 network, the dual-mode accuracy is improved by 0.5%, and compared with the original YOLOv8 network and the fused image, the accuracy is improved by 7.4%. Compared with RGB and NIR, the single-mode increases by 3.7% and 8.1% respectively. In terms of FPS, the improved Swin-T-YOLOv8+Slim-neck model and the single-mode NIR model perform best, reaching 120.The following Figure 4 shows the comparison of the training process of multiple models mAP0.5 and precision on the extended data set.

The experimental comparison is shown in Figure 4. According to the data in Figure 4a, the improved Swin-T-YOLOv8+Slim-neck model has great advantages compared with single-mode NIR and RGB images, and the accuracy of the network model without improvement using fusion images is further improved. At the same time, it can be seen from Figure 4b that the improved Swin-T-YOLOv8+Slim-neck model has better performance in stability and accuracy values. The effectiveness of our improved Swin-T YOLOv8 model for weed detection in complex field environments was verified. At the same time, these results also highlight the advantages of dual-mode image fusion and Swin-T-YOLOv8+Slim-neck model improvement in improving detection performance.

Detection and extraction of meristem position in weeds

Laser weeding technology is a method of using a high energy laser beam to accurately irradiate the growing point of weeds, and its purpose is to destroy the cell structure of weeds so as to achieve the effect of eliminating weeds. Determining the location of the weeds' growing points is crucial after weeds and crops have been identified (Marx *et al*., 2012). The early growth of a weed depends mainly on the continuous division and differentiation of its meristem cells, which are mainly concentrated in the growing points of

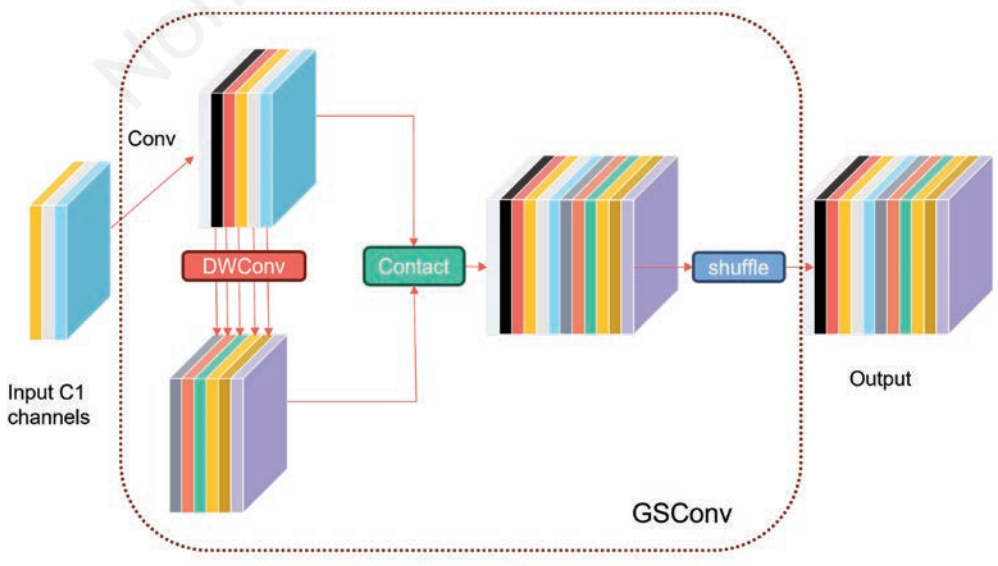

Figure 2. GSConv schematic diagram.

the weed, such as the stem tips and root tips. However, laser irradiation cannot directly affect root tips because they are typically found beneath the soil. Thus, laser weeding technology is mainly aimed at the stem tip of weeds.

In this study, the weed is eliminated by irradiating the growing point of the weed stem, and image processing technology is used to precisely extract the location of the weed stem's growing point. Only by accurately locating the growing point of the weed can we guarantee that the laser irradiation can destroy the meristem of the weed to the greatest extent so as to effectively eliminate the weed.

There are three steps in the process of weed detection: First, we use the two-scale image fusion method to fuse the real-time visible and infrared images; Second, we use the improved Swin-T-YOLOv8+Slim-neck network to detect crops and weeds, obtaining the classification and location of weeds. Finally, the location of weed meristem is determined. Since weeds are typically distributed symmetrically in their young stage, we determine the central location of weeds by calculating the geometric center of the detected weed boundary box (as shown in Figure 5). This approach has a low computing complexity and minimal resource consumption, and it greatly improves laser weeding stability and accuracy. At the end, the calculated geometric center position is taken as the laser irradiation target point, as shown in step 3 in Figure 1.

Statistical experiment

To evaluate the efficiency of detection and laser irradiation of weed meristem using an automated laser weeding robot under field conditions prior to field trials. The experiment was carried out between five different maize rows, and the number of weeds in each row was different to meet the differences of field environment.

The collected data included the total number of weeds per row, the number of weeds effectively detected, and the number of effective weed meristem irradiated by the effective laser. The accuracy of weed detection and the efficiency of laser irradiation of weed meristem were calculated. The accuracy rate is calculated by dividing the number of weeds effectively detected by the total number of weeds, and the efficiency is calculated by dividing the number of weeds successfully irradiated by the laser into the number of weeds effectively detected.

Weeding robot control system

Software and hardware settings of the control system

The robot mobile platform is the carrier of two-mode weed detection and laser weed control. As shown in step 4 of Figure 1, based on prior research experience (Bawden *et al*., 2017), an electric-powered mobile platform for weeding robots is developed, which can be remotely controlled by an operator. The scalable platform is designed to conform to the actual growth width of the plant, and the distance between the two rounds can be adjusted at any time to adapt to the working conditions of varying plant distances.

The robot mobile platform, the vision inspection system, and the laser control system make up the three primary components of the mobile platform. The mobile platform is composed of two sides of the walking device, the overall body frame and the suspension device. To increase turning flexibility and reduce turning radius, the mobile platform is driven by two hub motors, the hub motor model SVD48V30A, which are located on the front wheels. The rear wheel is universal, and the platform steering is realized by the differential rotation of the two driving wheels. The overall drive system is powered by a ternary lithium battery (48V35Ah). The visual inspection system is responsible for the real-time detection and identification of weeds and crops in the field. The onboard laptop computer and depth camera D435i make up the visual inspection system, which is in charge of processing weed information and weed detection. It is possible to capture both visible and infrared images with the Intel Realsense camera D435i (Intel, USA). The camera has a focal length of 1.93 mm, and its parameters include maximum resolution, visible light sensor resolution and frame rate, and infrared resolution and frame rate. More specifically, the visible light sensor has a resolution and frame rate of 1920× 1080, 30 FPS (maximum), and the infrared resolution

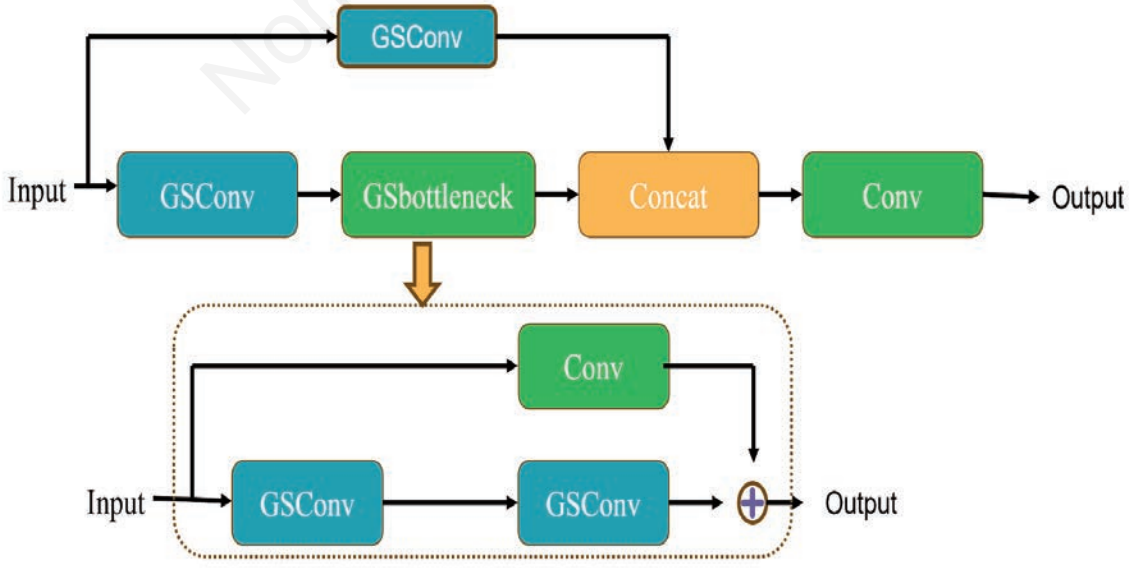

Figure 3. VoV-GSCSP structure diagram.

and frame rate of 1280× 720,90 FPS (maximum). The camera's shooting Angle is fixed, and the preset camera height is 46 cm. Two-modal image fusion technology and deep learning algorithm are used to improve the accuracy and efficiency of weed detection. The STMF407ZGT6 microcontroller serves as the primary control chip in the laser control system, enabling drive control of the laser actuator's data information and realization of analog-to-digital conversion. The controller is built around the ARM Cortex-M4 core, equipped with large capability flash and SARM, which performs well in digital signal control, image processing and other areas, and can adapt to the needs of field weeding. In addition, the laser control system also includes 15kHz AT15 scanning galvanometer, 405nm laser emitter, laser optical path layout board, laser driver, DAC8563 module, 220V power supply.

An automobile computer with the Ubuntu 20.04 operating system serves as the top computing device employed in this study, and its core control system is ROS (Noetic) installed in the operating system. The accuracy and real-time laser weeding are guaranteed by ROS, which communicates with each node through the way of publishing/subscribing messages, and each node is independent of each other, with a high degree of flexibility and scalability. Additionally, we may finish the fine-tuning of the Settings by making adjustments to the ROS system.

Control system flow

While the laser weeding process is automated, the operator moves the robot mobile platform remotely during the weeding operation phase. As shown in Figure 6, based on the improved Swin-T YOLOv8 network model, the trained model file (.pt file) is deployed offline to the ROS system for the prediction of crop and weed images in the field. The real-time image data acquired by the camera is transmitted to the ROS system via USB, and the visible and infrared image information is released in the form of color/image_raw and infra1/image_raw topics.

A node named yolov8 is constructed for target detection. This node subscribes to the topic of taking and publishing pictures and receives image information in real time. Using the dual-scale image fusion method, the visible and infrared images are fused, and the fused images are then fed into the Yolov8 detection module. The weights obtained by training are used to predict the detection frame containing the type and location of crops and weeds. The geometric location center of the detection frame is computed based on the obtained weed detection frame, and the location information of the obtained weed center is published in the detection topic. Subsequently, a node named center_listener is established in order to subscribe to the topic and forward the received messages over the serial port. After receiving the messages from the serial

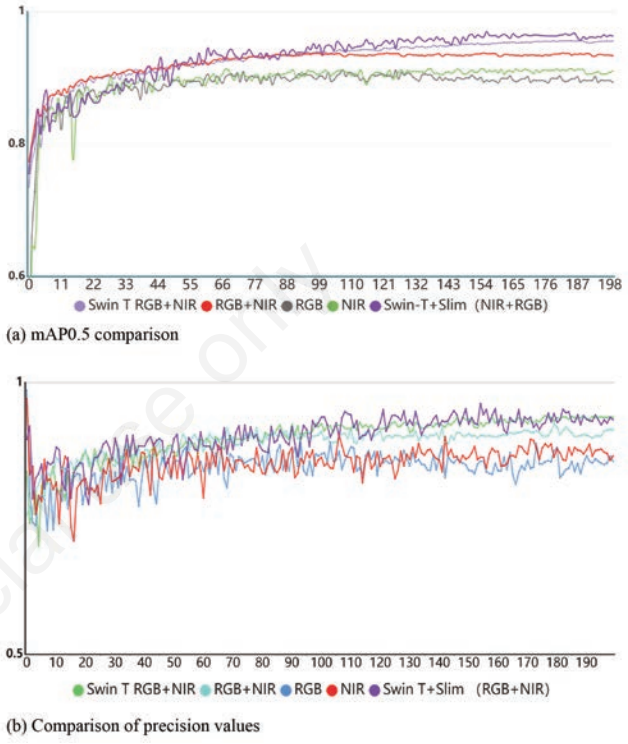

Figure 4. Comparison of the training processes of multiple models mAP0.5 and precision on the extended dataset.

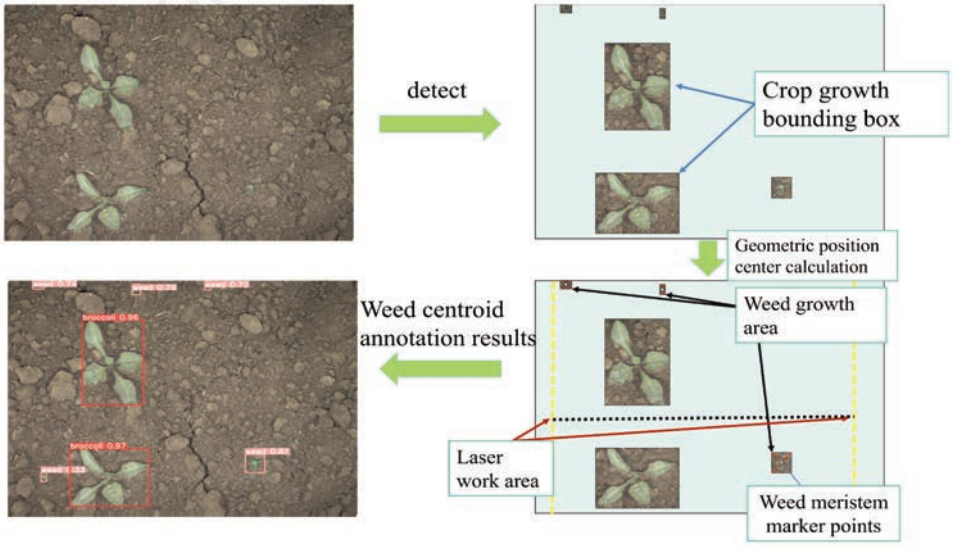

Figure 5. Weed meristem labeling process.

port, the STM32 device processes these messages through the internal program, and transmits the processed signal to the laser control system through the DAC8563 module. Finally, the laser control system performs accurate weeding operations based on these signals. When the geometric position center of the weed is detected, the laser polarization device aligns itself with the geometric position center of the weed. The main steps are as follows: (a) Receive the images taken by the depth camera D435i and fuse the resulting visible and infrared images; (b) Display the improved Swin-T YOLOv8 network to detect weed and crop classification results and detection boxes; (c) Calculate the geometric location center of the weed boundary box to determine the meristem location of the weed; (d) Publish the central location information of weeds through the node to the serial port; (e) The TTL-USB module receives the aforementioned data from the serial port; the STM32F407ZGT6 microcontroller processes it and forwards it to

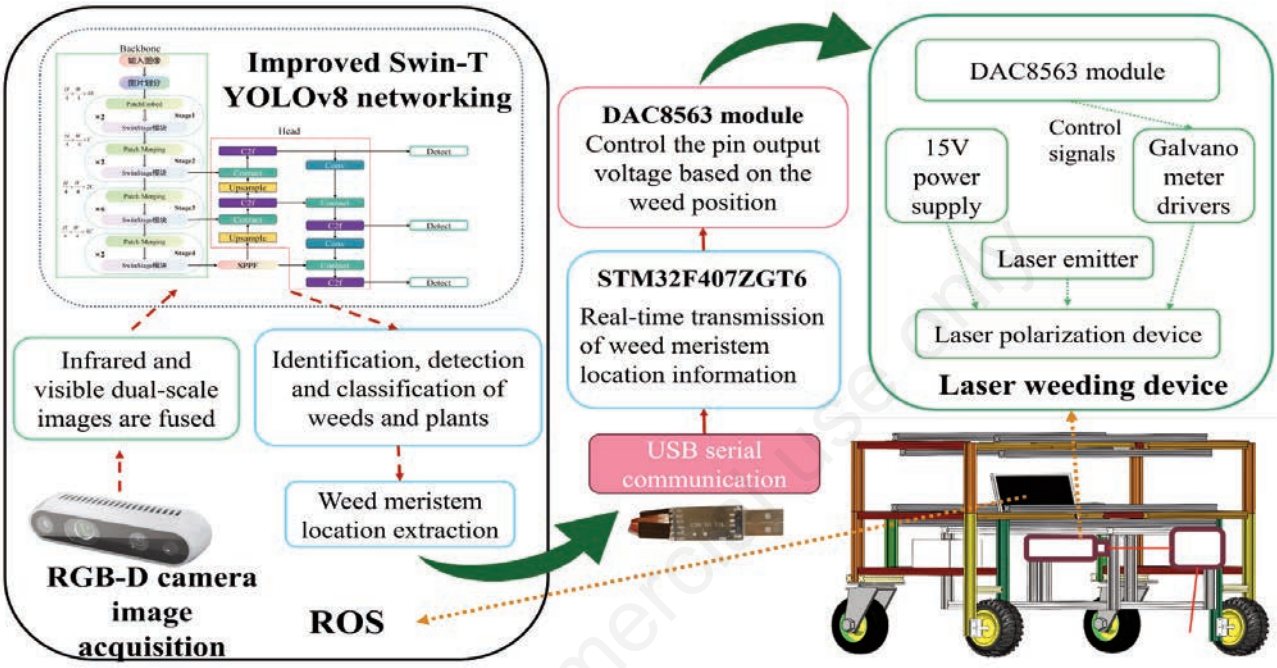

Figure 6. Overall control flow chart.

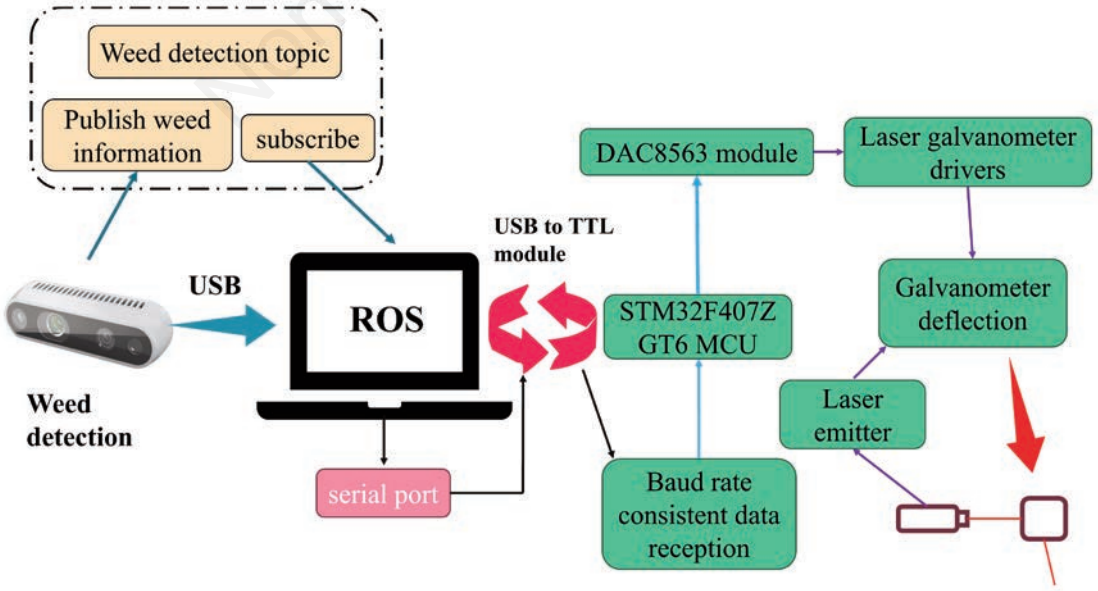

Figure 7. ROS system control flowchart and working principle diagram.

the DAC8563-SPI module, which then transmits a signal to control the laser galvanometer's deflection; (f) After controlling the laser scope deflection of one weed unit, go to the next weed location and repeat the above operation. Figure 7 below shows the ROS system control flow chart and working principle diagram.

Design of weed detection nodes

In our automatic weeding system, a ROs-based multi-node architecture is designed to achieve efficient communication and collaboration between components. First, create a ROS topic called weed_detection for communication between the depth camera and the ROS system. Offline training files, tag files, and API libraries will all be covered in this topic. Next, start the yolov8_ros node and run the yolo_v8.py file, which is responsible for receiving images from the depth camera. This node subscribes to the topic /camera/color/image_raw and /camera/infra1/image_raw to obtain the image information released by the D435i camera and completes the fusion of dual-mode images. The pre-trained Swin-T YOLOv8 weight model (.pt file) is used to detect and process the image. The detected image information is made available to the yolov8/center topic, which contains the geometric location and center location information of several weeds. The center_listener node is used to subscribe to the topic and simultaneously provide data to the serial port. Through the collaboration of multiple nodes and topics, the ROS system enables the completion of the entire process, from image acquisition by depth camera to weed detection using the improved model, then to publishing the detection results and processing the central information of weeds, as shown in Figure 8.

Laser control node design

In the automatic laser weeding system, the laser control node receives the central location information of multiple weeds from

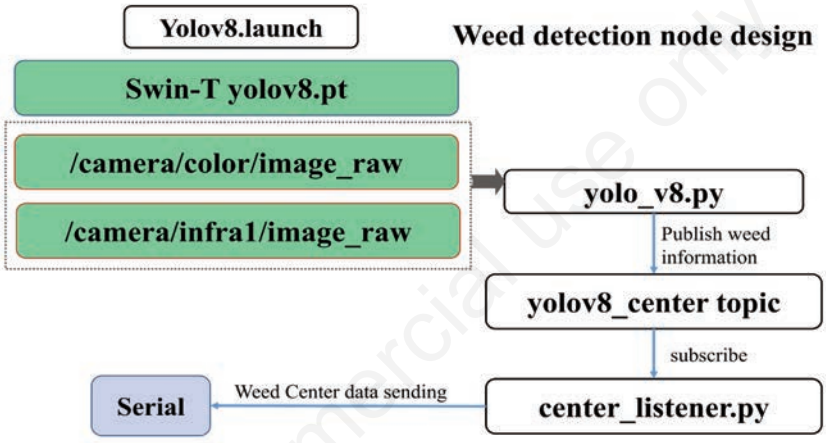

Figure 8. Detection node design.

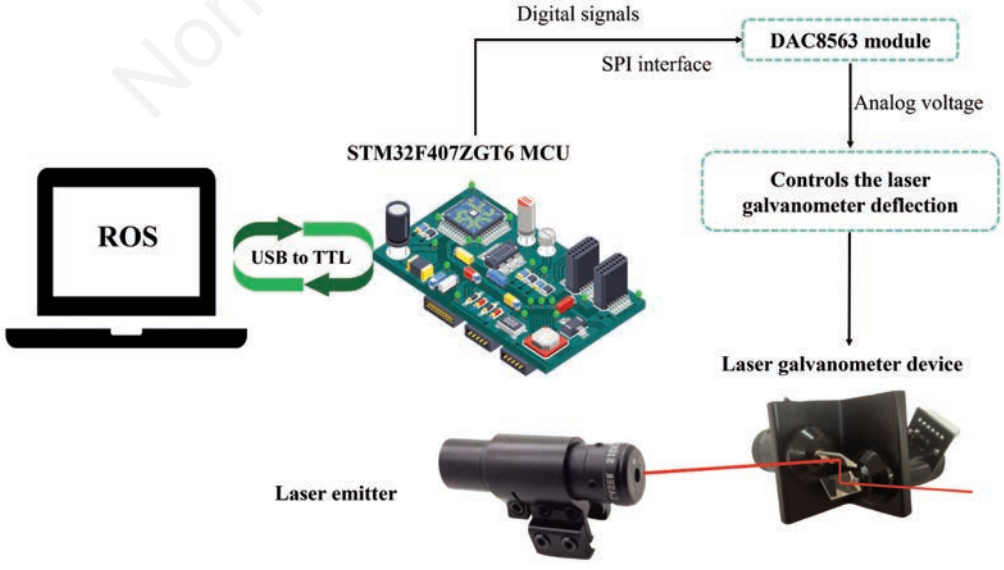

Figure 9. Laser control flowchart.

the serial port: Through the use of a USB serial port, the ROS system communicates with an STM32 microcontroller, which receives and processes the information in real time. The STM32 microcontroller then controls the output of the digital analog converter (DAC) in accordance with these data, and the DAC converts the information into a voltage signal, thus controlling the rotation of the laser galvanometer. The laser control flow chart is shown in Figure 9.

Laser galvanometer device

The laser weeding system mainly produces laser by laser emitter. The core components of the system include a 15kHz AT15 scanning galvanometer, a 405 nm laser transmitter, a laser optical path layout board, a laser driver, and a DAC8563 module with an SPI interface.

Field weeding requirements can be addressed by the 15kHz AT15 scanning galvanometer, which can swiftly and precisely alter the direction of the laser beam to cover the entire field within a -20° to 20° polarization angle range. The DAC8563 module is responsible for converting the incoming digital signal into an analog signal to control the movement of the galvanometer, and this conversion process enables the system to precisely control the direction of the laser beam. To guarantee precise laser transmission, a stable laser optical path is constructed using the laser optical path layout board. The laser driver provides a high voltage to the laser galvanometer device, allowing it to control the galvanometer rotation in response to voltage variations. In the process of laser weeding, when the weeding device moves above the weed, the system first controls the laser scope to deflect a specific Angle according to the position information of the weed meristem. Next, it activates the laser emitter to emit light, adjusting the laser's position irradiation based on the real-time information received, allowing for the precise removal of each weed. The hardware connection of the laser weeding device is shown in Figure 10.

Results and Discussion

Control of robot vision system

The mismatch of relative location information between the visible image and the infrared image captured by the depth camera is a concern. To address this issue, a feature-based image registration method is used to align the infrared image with the visible image. This guarantees the consistency of the weed location data obtained from the visible and infrared images. The camera is calibrated to make sure the laser scope can accurately illuminate the location of the weed meristem that the depth camera detected. First, 20 sets of data are measured at the location of the laser irradiation using a calibration plate, which contain the location of the calibration board in both the image coordinate system and the world coordinate system. The transformation relationship between the image coordinate system and the world coordinate system is computed and the internal and external camera parameters are derived by comparing these positions in the two coordinate systems. Through these parameters, the weed meristem locations identified by the depth camera can be accurately mapped to the irradiation location of the laser galvanometer to achieve accurate laser irradiation.

Laser control system regulation

Since precise laser control is essential for eliminating weeds, the magnitude of the different voltage amplituaries in the laser polarization device of the laser weeding robot is collected. Since the location of laser irradiation is related to the height from the ground, the height of the laser polarization device was set to 50cm and the height from the target weed was 46cm to analyze the error relationship between the output voltage and the location of laser irradiation. The experimental results show that when the output voltage reaches 4V, the laser galvanometer reaches its maximum deflection Angle, that is, 20°. In addition, the experiment also shows that the deflection Angle of the galvanometer decreases linearly with the decrease of voltage. Since the relation between voltage input and deflection Angle of galvanometer is definite, the relation between deflection Angle and position distance is obtained by measuring the position of laser irradiation at different angles. The laser irradiation distance is compensated for the set voltage value, and by lowering the corresponding voltage value, the relationship between the corrected distance and the voltage output is obtained.

Field trials of laser weeding robots

The built laser weeding robot was tested in a standard field, and the experimental results were collected and classified. The field experiment was carried out in the maize planting field of Kexin Agricultural Base in Jinghai District, Tianjin. The experimental conditions were as follows: maize seedlings and weeds

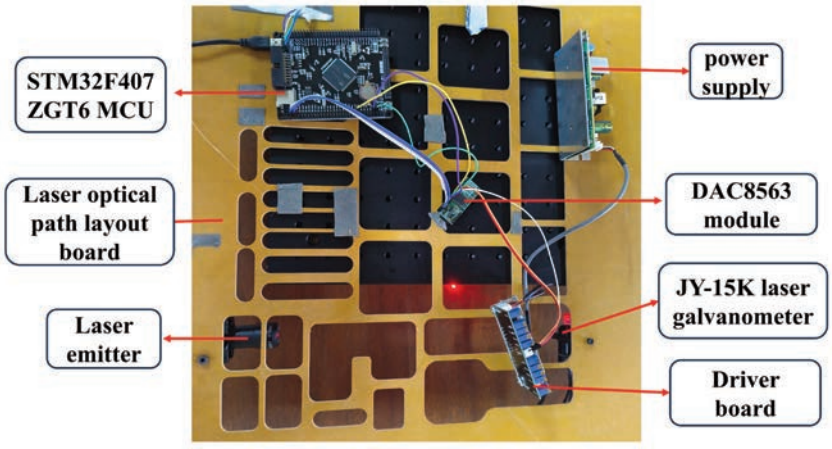

Figure 10. Laser hardware connection diagram.

existing in the three to five leaf stage of maize were planted in flat cropping mode, with row spacing of 60 cm, plant spacing of 25 cm, and crop height of 20-30 cm. The weather is fine, 28~35°C, the southeast wind is 2, and the precipitation of this month is 0 as of the experiment day. The camera is mounted in the center of the platform chassis through the jig, 46 cm from the ground. Because the field light intensity is too strong, so the use of shading cloth to reduce the light to meet the requirements of the experiment. The field test of the weeding robot is shown in Figure 11. The platform is built with 40×40 European standard aluminum profiles. The front wheels are driven by wheel hub motors and powered by ternary lithium batteries. The rear wheels are equipped with universal wheels, which work together with the front wheels. Steering is achieved by the differential rotation of the front wheel hub motor controlled by the SVD48V50A motor driver. This paper studies the use of manual control to adjust the direction through the dual drive remote control and its signal receiver. The built laser weeding robot was tested in a standard field, and the experimental results were collected and classified. The field experiment was carried out in the maize planting field of Kexin Agricultural Base in Jinghai District, Tianjin. The experimental conditions were as follows: maize seedlings and weeds existing in the three to five leaf stage of maize were planted in flat cropping mode, with row spacing of 60 cm, plant spacing of 25 cm, and crop height of 20-30 cm. The weather is fine, 28~35°C, the southeast wind is 2, and the precipitation of this month is 0 as of the experiment day. The camera is mounted in the center of the platform chassis through the jig, 46 cm from the ground. Because the field light intensity is too strong, so the use of shading cloth to reduce the light to meet the requirements of the experiment. The field test of the weeding robot is shown in Figure 11. The platform is built with 40×40 European standard aluminum profiles. The front wheels are driven by wheel hub motors and powered by ternary lithium batteries. The rear wheels are equipped with universal wheels, which work together with the front wheels. Steering is achieved by the differential rotation of the front wheel hub motor controlled by the SVD48V50A motor driver. This paper studies the use of manual control to adjust the direction through the dual drive remote control and its signal receiver. In the operating state, the depth camera is installed in the abdomen of the mobile platform through the connector, and the laser device is installed in the tail of the mobile platform. Weeds and crops first pass through the field of view area of the camera, and then reach the treatment area of the laser weeding device, detect and obtain the location of weed meristem, and guide the laser weeding device to treat the corresponding area. In addition, the proficiency of a laser weeding robot's identification abilities is assessed. In this paper, a "stop-and-go" moving mode is used to control the robot walking, and the robot stops moving when controlling the laser weeding. In order to improve the efficiency of laser weeding, it is necessary to avoid the problem that the laser polarization device and moving platform can not accurately point to the center of the weeds when they are moving. The laser polarization device is controlled at a distance of 50cm from the ground and 46cm from weeds. The main body of the image acquisition device is an aluminum alloy rectangular frame composed of 40×40 European standard profiles. In order to reduce the influence of weed exposure factors caused by direct sunlight and strong light on the weeding effect, a blackout screen is used to shield the camera and laser weeding components to improve the accuracy of weed detection. The research uses a blackout cloth to cover the frame and form a black box to isolate the sunlight in the identification area. The black box opens front and back to pass through the crop and weed plants, and is equipped with 8 sets of LED lights to provide a stable light source. In the middle area of the light source, the D435i depth camera is installed as the core component of the image acquisition device. The frame length is 180 cm, the width perpendicular to the forward direction is 54 cm, and the camera field of view is 36×46 cm. The depth camera, D435i, captures images with a resolution of 384x480 pixels and a frame rate of about 20FPS. According to the results of statistical experiment Table 3, under field conditions, the total number of weeds in the detection area was 206, the number of effective detected weeds was 170, the accuracy rate of weed detection was 82.1%, the total number of effective detected weed meristem locations was 122,

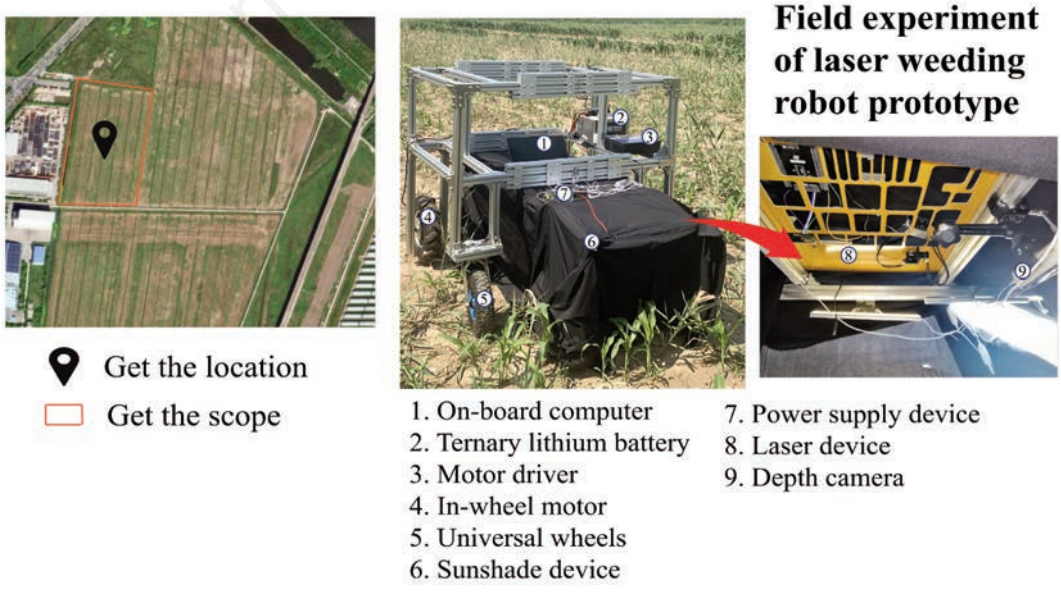

Figure 11. Field images of laser weeding robot.

and the accuracy rate of effective simulation laser was 72.3%, which was lower than the accuracy of laboratory training results. On the one hand, large random interference has a high impact on model detection, on the other hand, ground fluctuation reduces the recognition and laser aiming accuracy of the weeding robot. which is lower than the accuracy of the training results in the lab. Finally, due to the fluctuation of speed, the laser could not be irradiated in time after the detection of weeds, resulting in a low laser accuracy. Large random interference has a higher effect on model detection on the one hand, but ground fluctuation reduces the identification and laser pointing accuracy of weeding robots on the other. With its high detection performance and ability to eliminate interference from field environmental factors, the Swin-T yolov8 detection model based on image fusion can increase the accuracy of weed detection and fulfill the demands of precise laser control and field irradiation.

Therefore, in order to more clearly illustrate the irradiation position of laser weeding, three field test images with superior effects were chosen to display. The experimental images of the weeds being exposed to radiation during the field weeding procedure using a laser weeding robot are shown in Figure 12.

Conclusions and Future Prospects

In order to address the issues of low weed detection accuracy and poor anti-interference strength caused by environmental factors in field circumstances, as well as to encourage the employment of multi-modal image fusion and laser weed control technology in precision agriculture weed management, this study proposes a laser weed control robot based on dual-mode fusion weed detection. The three primary components of the research are the fusion of infrared and visible images, the improvement of the YOLOv8 network model structure, and the control of the laser polarization device. The two-mode fusion technique of fusing visible and infrared images adopts the two-scale fusion method of pixel-level fusion to fuse the two. The experimental findings demonstrate that the method can significantly increase the accuracy of weed detection and improve the adaptability in various field scenarios when compared to the results of image training in single mode. We improve the YOLOv8 model to increase the accuracy of weed detection for small target weeds. The outcomes demonstrate that the improved Swin-T-YOLOv8+Slim-neck has higher accuracy in detecting small target weeds with a weed detection efficiency of 96.0%. On this basis, this study designs and builds an intelligent laser weeding robot, which deploys image fusion, weed detection, intelligent control and other technologies. Through machine vision detection and positioning of the geometric position center of weeds, an efficient laser weeding method is realized. Under field conditions, the accuracy rate for weed detection is 82.1%, and the effective simulation rate for laser removal is 72.3%. The experimental results show that the application of the above method can accurately point the location of weed meristem, solve the problem of low precision and poor robustness of weed detection by various factors, and provide an advanced method for field target detection. In addition, the laser weeding method also provides an optional method for field cleaning and precise weeding.

This method meets the requirements of precision and environmental protection in field weeding. In recent years, the research of multimodal image fusion and laser irradiation technology has been deepening, and the technology has gradually become mature and stable. There is a growing demand for such technologies in the agricultural sector, especially in smart and precision agriculture. In the field of agricultural weeding commercialization in the future, multi-mode laser weeding robots will certainly promote the process of intelligent weeding technology.

The laser weeding robot still has certain limitations, despite the improved model's partial success in achieving high precision: it lacks a comprehensive robot system that integrates detection, nav-

Figure 12. Location diagram of weed meristem of three different weeds irradiated by laser in the field.

Table 3. Statistical experiments of weeds irradiated by laser.

Corn row number	Number of weeds	Number of weeds effectively detected	Average accuracy of weed detection	Effective monitoring sites of weed meristem	Effective laser removal rate
1	52	170	82.1%	31	72.3%
2	41			27	
3	31			18	
4	38			24	
5	44			22	

igation, and control, thus some manual involvement is still necessary. In addition, the laser control device subject to experimental conditions can also improve the precision and efficiency of weeding. Subsequent research endeavors may explore the incorporation of cross-modal imagery to address the challenges involved in weed detection more thoroughly. Simultaneously, when the impact on weed detection efficiency is minimal, we can combine the data that comprehensively conveys weed features in order to enhance weed detection efficiency. A laser control system with adjustable laser energy is studied to emit different laser energies in different weeds and different growth periods to remove weeds more efficiently.

References

Ahmad, J., Muhammad, K., Ahmad, I., Ahmad, W., Smith, M.L., Smith, L.N., et al. 2018. Visual features based boosted classification of weeds for real-time selective herbicide sprayer systems. Comput. Ind. 98:23-33.

Arsa, D.M.S., Ilyas, T., Park, S.-H., Won, O., Kim, H. 2023. Eco-friendly weeding through precise detection of growing points via efficient multi-branch convolutional neural networks. Comput. Electron. Agr. 209:107830.

Bavirisetti, D.P., Dhuli, R., 2016. Two-scale image fusion of visible and infrared images using saliency detection. Infrared Phys. Technol. 76:52–64.

Bawden, O., Kulk, J., Russell, R., McCool, C., English, A., Dayoub, F., et al. 2017. Robot for weed species plant-specific management: BAWDEN *et al*. J. Field Robot. 34:1179-1199.

Bwambale, E., Abagale, F.K., Anornu, G.K., 2022. Smart irrigation monitoring and control strategies for improving water use efficiency in precision agriculture: A review. Agr. Water Manage. 260:107324.

Cheng, X., Geng, K., Wang, Z., Wang, J., Sun, Y., Ding, P., 2023. SLBAF-Net: Super-Lightweight bimodal adaptive fusion network for UAV detection in low recognition environment. Multimed. Tools Appl. 82:47773-47792.

Cisternas, I., Velásquez, I., Caro, A., Rodríguez, A., 2020. Systematic literature review of implementations of precision agriculture. Comp. Electron. Agr. 176:105626.

Espejo-Garcia, B., Panoutsopoulos, H., Anastasiou, E., Rodríguez-Rigueiro, F.J., Fountas, S., 2023. Top-tuning on transformers and data augmentation transferring for boosting the performance of weed identification. Comp. Electron. Agr. 211:108055.

Fahad, S., Hussain, S., Chauhan, B.S., Saud, S., Wu, C., Hassan, S., Tanveer, M., Jan, A., Huang, J., 2015. Weed growth and crop yield loss in wheat as influenced by row spacing and weed emergence times. Crop Protect. 71:101–108.

Gai, J., Tang, L., Steward, B.L., 2020. Automated crop plant detection based on the fusion of color and depth images for robotic weed control. J. Field Robot. 37:35–52.

Gan, H., Lee, W.S., Alchanatis, V., Ehsani, R., Schueller, J.K., 2018. Immature green citrus fruit detection using color and thermal images. Comp. Electron. Agr. 152:117–125.

Jiang, W., Quan, L., Wei, G., Chang, C., Geng, T., 2023. A conceptual evaluation of a weed control method with post-damage application of herbicides: A composite intelligent intra-row weeding robot. Soil Till. Res. 234:105837.

Li, D., Li, B., Long, S., Feng, H., Wang, Y., Wang, J., 2023. Robust detection of headland boundary in paddy fields from continuous RGB-D images using hybrid deep neural networks. Comp. Electron. Agr. 207:107713.

Li, D., Song, Z., Quan, C., Xu, X., Liu, C., 2021. Recent advances in image fusion technology in agriculture. Comp. Electron. Agr. 191:106491.

Li, H., Wu, X.-J., 2019. DenseFuse: a fusion approach to infrared and visible images. IEEE T. Image Process 28:2614–2623.

Ma, J., Ma, Y., Li, C., 2019. Infrared and visible image fusion methods and applications: A survey. Inform. Fusion 45:153–178.

Machleb, J., Peteinatos, G.G., Kollenda, B.L., Andújar, D., Gerhards, R., 2020. Sensor-based mechanical weed control: Present state and prospects. Comput. Electron. Agr. 176:105638.

Martelloni, L., Frasconi, C., Sportelli, M., Fontanelli, M., Raffaelli, M., Peruzzi, A., 2020. Flaming, Glyphosate, hot foam and nonanoic acid for weed control: a comparison. Agronomy. 10:129.

Marx, C., Barcikowski, S., Hustedt, M., Haferkamp, H., Rath, T., 2012. Design and application of a weed damage model for laser-based weed control. Biosyst. Eng. 113:148–157.

Mathiassen, S.K., Bak, T., Christensen, S., Kudsk, P., 2006. The effect of laser treatment as a weed control method. Biosyst. Eng. 95:497–505.

Pérez-Ruíz, M., Slaughter, D.C., Fathallah, F.A., Gliever, C.J., Miller, B.J., 2014. Co-robotic intra-row weed control system. Biosyst. Eng. 126:45–55.

Quan, L., Jiang, W., Li, H., Li, H., Wang, Q., Chen, L., 2022. Intelligent intra-row robotic weeding system combining deep learning technology with a targeted weeding mode. Biosyst. Eng. 216:13–31.

Raja, R., Nguyen, T.T., Slaughter, D.C., Fennimore, S.A., 2020. Real-time weed-crop classification and localisation technique for robotic weed control in lettuce. Biosyst. Eng. 192:257–274.

Rani, L., Thapa, K., Kanojia, N., Sharma, N., Singh, S., Grewal, A.S., et al. 2021. An extensive review on the consequences of chemical pesticides on human health and environment. J. Cleaner Prod. 283:124657.

Sujaritha, M., Annadurai, S., Satheeshkumar, J., Kowshik Sharan, S., Mahesh, L., 2017. Weed detecting robot in sugarcane fields using fuzzy real time classifier. Comput. Electron. Agr. 134:160–171.

Tu, S., Pang, J., Liu, H., Zhuang, N., Chen, Y., Zheng, C., W., et al. 2020. Passion fruit detection and counting based on multiple scale faster R-CNN using RGB-D images. Precision Agric. 21:1072–1091.

Wang, A., Zhang, W., Wei, X., 2019. A review on weed detection using ground-based machine vision and image processing techniques. Comput. Electron. Agr. 158:226–240.

Wang, M., Leal-Naranjo, J.-A., Ceccarelli, M., Blackmore, S., 2022. A novel two-degree-of-freedom gimbal for dynamic laser weeding: design, analysis, and experimentation. IEEE/ASME Trans. Mechatron. 27:5016–5026.

Wang, Y., Zhang, S., Dai, B., Yang, S., Song, H., 2023. Fine-grained weed recognition using Swin Transformer and two-stage transfer learning. Front. Plant Sci. 14:1134932.

Westwood, J.H., Charudattan, R., Duke, S.O., Fennimore, S.A., Marrone, P., Slaughter, D.C., et al. 2018. Weed management in 2050: perspectives on the future of weed science. Weed Sci. 66:275–285.

Wu, X., Aravecchia, S., Lottes, P., Stachniss, C., Pradalier, C., 2020. Robotic weed control using automated weed and crop classification. J. Field Robot. 37:322–340.

Xiong, Y., Ge, Y., Liang, Y., Blackmore, S., 2017. Development of

a prototype robot and fast path-planning algorithm for static laser weeding. Comput. Electron. Agr. 142:494–503.

Xu, K., Zhu, Y., Cao, W., Jiang, X., Jiang, Z., Li, S., Ni, J., 2021. Multi-Modal deep learning for weeds detection in wheat field based on RGB-D images. Front. Plant Sci. 12:732968.

Xue, Y., Ju, Z., Li, Y., Zhang, W., 2021. MAF-YOLO: Multi-modal attention fusion based YOLO for pedestrian detection. Infrared Phys. Technol. 118:103906.

Zhang, X., Ye, P., Leung, H., Gong, K., Xiao, G., 2020. Object fusion tracking based on visible and infrared images: A comprehensive review. Inform. Fusion 63:166–187.

Zhu, H., Zhang, Y., Mu, D., Bai, L., Zhuang, H., Li, H., 2022. YOLOX-based blue laser weeding robot in corn field. Front. Plant Sci. 13:1017803.

Zhu, J., Wang, J., DiTommaso, A., Zhang, C., Zheng, G., Liang, W., et al. 2020. Weed research status, challenges, and opportunities in China. Crop Protect. 134:104449.

Zou, K., Wang, H., Yuan, T., Zhang, C., 2023. Multi-species weed density assessment based on semantic segmentation neural network. Precis. Agric. 24:458–481.